Eur. Phys. J. D **41**, 55–59 (2007)
DOI: 10.1140/epjd/e2006-00206-0

THE EUROPEAN PHYSICAL JOURNAL D

Further experimental investigation of the hyperfine structure in the spectrum of atomic niobium

S. Kröger[a]

Institut für Atomare Physik und Fachdidaktik, Technische Universität Berlin, Hardenbergstr. 36, 10623 Berlin, Germany

Received 15 March 2006 / Received in final form 4 August 2006
Published online 13 September 2006 –

Abstract. Laser spectroscopy with either optogalvanic or laser induced fluorescence detection have been employed to measure the hyperfine structure of 25 transitions of atomic niobium in the visible and near infrared spectral range. The magnetic dipole hyperfine interaction constants A of 43 energy levels (22 of even and 21 of odd parity) were determined, 30 of which have been investigated for the first time. The values obtained for the even parity levels are compared with the results of a parametric analysis.

PACS. 32.30.Jc Visible and ultraviolet spectra – 31.30.Gs Hyperfine interactions and isotope effects, Jahn-Teller effect

1 Introduction

In recent years the fine and hyperfine structure of atomic niobium has been the subject of renewed interest [1–3]. An initial report [1] on experimental determination of the hyperfine structure constants of levels of the even configurations $4d^3 5s^2$, $4d^4 5s$, $4d^5$, $4d^4 6s$ and $4d^3 5s 6s$ and odd configurations $4d^4 5p$ and $4d^3 5s 5p$ using optogalvanic laser spectroscopy and laser induced fluorescence spectroscopy yields a comprehensive compilation of all known hyperfine structure data. Based on these experimental data, a second paper [2] reports in detail on a parametric analysis of the fine and hyperfine structure for all known even configurations. Therein core polarisation effects are discussed and theoretical predictions for the hyperfine interaction constants, A and B, for all levels of the configurations $4d^3 5s^2$, $4d^4 5s$ and $4d^5$ are given. Additionally, the existence of two fine structure levels as given in the Moore tables of atomic energy levels [4] were called into question. This matter required further experimental investigations, which led to the revision of four known and the inclusion of two new energy levels [3].

In this work, the hyperfine structures of 25 transitions of atomic niobium have been measured. The results of the evaluation are presented.

2 Experimental

Doppler-limited laser spectroscopy methods, with a tunable single-mode cw ring laser, were applied on Nb vapour for the determination of the hyperfine structure splitting of selected lines in the Nb I spectrum: laser induced fluorescence spectroscopy (lif) was used in the blue spectral range (470 nm to 510 nm with the laser dye Coumarin 102) and optogalvanic laser spectroscopy (ogs) in the red and near infrared spectral range (660 nm to 680 nm with the laser dye DCM and 905 nm to 925 nm with a titanium-sapphire laser). For the evaporation of the Nb metal and an efficient population of the lower levels of the lines under study a liquid nitrogen cooled hollow cathode lamp was used. Further details of the experimental set-up are given in reference [1].

Altogether 25 lines of atomic Nb have been investigated. They are listed in Table 1 inclusive classification and intensities as given in the NBS [5] and the MIT [6] wavelength tables. Additionally, the wavelength of at least one of the fluorescence lines is given for the lines measured by lif.

Three of the lines in Table 1 are not listed in the standard references [5,6] and are proven to be transitions to new levels as reported in reference [3]. At the wavelength of 502.63 nm, two lines lie in close proximity, so that the hyperfine spectra of both overlap, and it was necessary to use lif to record them separately.

3 Results and discussion

The 25 transitions combine 22 different levels of even parity with 21 different levels of odd parity. Each line has been recorded and fitted ten times. For the determination of the hyperfine interaction constants, the spectra were fitted with Voigt profile functions using the following fit parameters: the centre of gravity of the hyperfine structure, the A and B constants of the upper and lower level,

[a] e-mail: sk@kalium.physik.tu-berlin.de

Table 1. Nb I transitions investigated by means of optogalvanic spectroscopy (ogs) or by means of laser induced fluorescence spectroscopy (lif); in the last column the fluorescence wavelength λ_f is given for the lif measurements; intensities I according to [5,6].

		I	log(I)	lower level			upper level			
λ_{air}/nm	σ/cm^{-1}	[5]	[6]	E/cm^{-1}	config.	term	E/cm^{-1}	config.	term	λ_f/nm
470.830	21 233.16	260	1.7	17 405.32	$4d^3 5s5p$	$^6G_{7/2}$	38 638.47	$4d^3 5s6s$	$^6F_{7/2}$	545.62
471.579	21 199.41	65	0.5	16 672.00	$4d^3 5s5p$	$^6G_{3/2}$	37 871.30	$4d^3 5s6s$	$^6F_{1/2}$	547.87
472.378	21 163.58	55	0.7	17 937.26	$4d^3 5s5p$	$^6G_{9/2}$	39 100.73	$4d^3 5s6s$	$^6F_{9/2}$	521.12
474.240	21 080.49			18 568.18	$4d^3 5s5p$	$^6G_{11/2}$	39 648.67	$4d^3 5s6s$	$^6F_{11/2}$	528.54
474.968	21 048.15	220	2.0	11 524.65	$4d^4 5s$	$^4H_{13/2}$	32 572.72	$4d^3 5s5p$	$^4G_{11/2}$	335.84
475.141	21 040.49	65	0.5	16 981.01	$4d^3 5s5p$	$^6G_{5/2}$	38 021.41	$4d^3 5s6s$	$^6F_{3/2}$	543.40
476.678	20 972.65	65	0.7	17 476.22	$4d^4 5s$	$^2H_{11/2}$	38 448.77	$4d^3 5s5p$	$^2H_{9/2}$	379.45
478.994	20 871.27	65	0.7	17 405.32	$4d^3 5s5p$	$^6G_{7/2}$	38 276.59	$4d^3 5s6s$	$^6F_{5/2}$	546.81
483.760	20 665.62	26	0.7	12 136.86	$4d^4 5s$	$^4G_{7/2}$	32 802.44	$4d^4 5p$	$^4G_{9/2}$	504.40
486.896	20 532.55	80	1.0	18 568.18	$4d^3 5s5p$	$^6G_{11/2}$	39 100.73	$4d^3 5s6s$	$^6F_{9/2}$	521.12
491.092	20 357.10	80	1.2	19 291.57	$4d^3 5s5p$	$^6G_{13/2}$	39 648.67	$4d^3 5s6s$	$^6F_{11/2}$	534.36
499.429	20 017.29	65	0.7	10 922.74	$4d^4 5s$	$^4H_{7/2}$	30 940.02		$J = 9/2$	573.74
502.475	19 895.94			11 044.08	$4d^4 5s$	$^4H_{9/2}$	30 940.02		$J = 9/2$	573.74
502.634	19 889.66	150	1.7	1 050.26	$4d^4 5s$	$^6D_{9/2}$	20 939.92	$4d^3 5s5p$	$^6F_{11/2}$	551.28
502.637	19 889.53			12 018.25	$4d^4 5s$	$^4G_{5/2}$	31 907.74	$4d^4 5p$	$^4F_{3/2}$	430.87
507.676	19 692.13			11 247.88	$4d^4 5s$	$^4H_{11/2}$	30 940.02		$J = 9/2$	573.74
661.415	15 114.90	35	1.4	8 410.90	$4d^4 5s$	$^4D_{1/2}$	23 525.80	$4d^4 5p$	$^2D_{3/2}$	ogs
672.196	14 872.52		0.3	5 965.45	$4d^3 5s^2$	$^4P_{5/2}$	20 837.98	$4d^3 5s5p$	$^4D_{5/2}$	ogs
908.486	11 004.31		0.8	12 018.25	$4d^4 5s$	$^4G_{5/2}$	23 022.56	$4d^3 5s5p$	$^4G_{7/2}$	ogs
912.507	10 955.62		1.0	12 288.25	$4d^4 5s$	$^4F_{5/2}$	23 243.87	$4d^3 5s5p$	$^4F_{5/2}$	ogs
912.938	10 950.64		1.0	9 043.14	$4d^4 5s$	$^4D_{5/2}$	19 993.78	$4d^3 5s5p$	$^6F_{5/2}$	ogs
914.131	10 936.35		1.7	16 918.78	$4d^4 5s$	$^2G_{7/2}$	27 855.13	$4d^3 5s5p$	$^2G_{7/2}$	ogs
918.695	10 882.02		1.3	12 692.12	$4d^4 5s$	$^4F_{5/2}$	23 574.14	$4d^3 5s5p$	$^4F_{5/2}$	ogs
919.762	10 869.40		1.2	13 145.71	$4d^4 5s$	$^4F_{9/2}$	24 015.11	$4d^3 5s5p$	$^4F_{7/2}$	ogs
924.130	10 818.22		1.0	9 497.52	$4d^4 5s$	$^4D_{7/2}$	20 315.74	$4d^3 5s5p$	$^6D_{7/2}$	ogs

the Gaussian and Lorentzian part of the Voigt profile and two parameters to take into account background and slope of the background.

Due to the very small nuclear electric quadrupole moment of the only stable isotope ^{93}Nb, the contribution of the electric quadrupole hyperfine structure to the total splitting is very small. Therefore an accurate determination of the electric hyperfine interaction constant B using Doppler-limited experimental methods is difficult. This is especially problematic if the hyperfine structure is not completely resolved, which is the case for most of the investigated lines. The range of the resulting B values from the different fits of one line is mostly greater than the B value it self, and therefore no results for the B constants are given.

In contrast to the electric quadrupole moment, the nuclear magnetic dipole moment is large and in many transitions it is adequate to apply Doppler limited experimental techniques to determine accurately the magnetic hyperfine interaction constants A. These are listed in Table 2 for the levels of even parity and in Table 3 for the levels of odd parity. The A values are averaged over all fits and the error margins are the standard deviations, except for the cases which are discussed below.

For all lines a departure from the theoretical intensity ratios of the hyperfine structure components is found. The main reason for this is a saturation of the strong hyperfine components by the high laser intensity. This saturation results in an intensity limitation and broadening of the strong hyperfine components, which leads to an apparent relative intensity increase of the weak components. This effect is already discussed in reference [1] and is the reason that all spectra with well separated hyperfine components are fitted with individual profile and intensity parameters for each hyperfine component. Many of the investigated lines, especially transitions between levels with higher J values, are not completely resolved. For these lines the deviation of the theoretical intensity ratios is taken into account by fixing the intensity ratios according to the fit results of other lines. Different broadening for the individual hyperfine components has been accounted for, too.

In case one of the combining levels has a small hyperfine splitting (i.e. $A < 100$ MHz) particular difficulties in determining its hyperfine constant arise. With a line width of approximately 500 to 1 000 MHz (depending on the wavelength) due to the Doppler-limited laser spectroscopic method, it was not possible to resolve component pairs whose frequency differences reflect the hyperfine splitting of the weakly splitting level. Therefore, a precise determination of the hyperfine interaction constants of these levels was not possible. The only statement, which can be given for these levels, is that the A constant is approximately zero. The precision (i.e. the margin of error given in Tabs. 2 and 3) depends on the line width

Table 2. Experimental magnetic dipole hyperfine structure constants A of the levels of even parity of Nb I together with comparative values form literature [1,7–10] (values without reference are values determined in this work); the wavelength given in column 3 specifies the line which was used to determine the A values (abmr: atomic beam magnetic resonance).

E/cm^{-1}	level	λ_{air}/nm	A/MHz	Ref.
1 050.26	$4d^4 5s\ {}^6\mathrm{D}_{9/2}$	502.634	694 (4)	
		abmr	691.6141 (22)	[7]
5 965.45	$4d^3 5s^2\ {}^4\mathrm{P}_{5/2}$	672.19	340 (6)	
		643.046	343.4 (1.1)	[1]
		586.643	343.1670 (5)	[8]
		586.643	341.3 (10.0)	[9]
8 410.90	$4d^4 5s\ {}^4\mathrm{D}_{1/2}$	661.415	2 003 (11)	
		570.647	1 997.0 (1.1)	[8]
		570.647	2 001.7 (10.0)	[9]
9 043.14	$4d^4 5s\ {}^4\mathrm{D}_{5/2}$	912.938	–407 (3)	
		587.467	–407.8606 (43)	[8]
		583.860	–408.6 (10.0)	[9]
9 497.52	$4d^4 5s\ {}^4\mathrm{D}_{7/2}$	924.130	–478 (3)	
		591.943	–477.0373 (35)	[8]
		590.057	–474.4 (2.0)	[10]
		654.461	–477.3 (1.8)	[1]
		670.988	–478.0 (1.7)	[1]
		832.093	–476.9 (6)	[1]
		666.084	–475 (2)	[1]
10 922.74	$4d^4 5s\ {}^4\mathrm{H}_{7/2}$	499.429	–200 (50)*	
11 044.08	$4d^4 5s\ {}^4\mathrm{H}_{9/2}$	502.475	334 (50)*	
11 247.88	$4d^4 5s\ {}^4\mathrm{H}_{11/2}$	507.676	560 (30)*	
11 524.65	$4d^4 5s\ {}^4\mathrm{H}_{13/2}$	474.968	662 (20)*	
12 018.25	$4d^4 5s\ {}^4\mathrm{G}_{5/2}$	502.637	0 (80)*	
		908.486	–70 (40)*	
		581.533	–101.2 (6.0)	[10]
12 136.86	$4d^4 5s\ {}^4\mathrm{G}_{7/2}$	483.760	502.4 (1.4)	
12 288.25	$4d^4 5s\ {}^4\mathrm{F}_{3/2}$	912.507	–590 (30)*	
12 692.12	$4d^4 5s\ {}^4\mathrm{F}_{5/2}$	918.695	338.5 (8)	
13 145.71	$4d^4 5s\ {}^4\mathrm{F}_{9/2}$	919.762	667 (5)	
16 918.78	$4d^4 5s\ {}^2\mathrm{G}_{7/2}$	914.131	–86.3 (5)	
17 476.22	$4d^4 5s\ {}^2\mathrm{H}_{11/2}$	476.678	–20 (50)*	
37 871.30	$4d^3 5s6s\ {}^6\mathrm{F}_{1/2}$	471.579	–1 750.6 (1.4)	
		833.695	–1 749.9 (5)	[1]
38 021.41	$4d^3 5s6s\ {}^6\mathrm{F}_{3/2}$	475.141	556 (10)	
		823.388	547.7 (6)	[1]
38 276.59	$4d^3 5s6s\ {}^6\mathrm{F}_{5/2}$	478.994	868 (4)	
		818.807	871.9 (1.0)	[1]
38 638.47	$4d^3 5s6s\ {}^6\mathrm{F}_{7/2}$	470.830	955 (5)	
		846.790	958.5 (8)	[1]
39 100.73	$4d^3 5s6s\ {}^6\mathrm{F}_{9/2}$	472.378	983 (3)	
		486.896	985 (4)	
		855.850	981.8 (7)	[1]
39 648.67	$4d^3 5s6s\ {}^6\mathrm{F}_{11/2}$	474.240	994 (2)	
		491.092	994 (3)	

* B constants of both levels fixed during the fit.

Table 3. Experimental magnetic dipole hyperfine structure constants A of the levels of odd parity of Nb I together with comparative values form literature [1,10] (values without reference are values determined in this work); the wavelength given in column 3 specifies the line which was used to determine the A values.

E/cm^{-1}	level	λ_{air}/nm	A/MHz	Ref.
16 672.00	$4d^3 5s5p\ {}^6\mathrm{G}_{3/2}$	471.579	–339.1 (1.0)	
16 981.01	$4d^3 5s5p\ {}^6\mathrm{G}_{5/2}$	475.141	386 (10)	
17 405.32	$4d^3 5s5p\ {}^6\mathrm{G}_{7/2}$	470.830	601 (3)	
		478.994	601 (4)	
17 937.26	$4d^3 5s5p\ {}^6\mathrm{G}_{9/2}$	472.378	687.8 (1.5)	
18 568.18	$4d^3 5s5p\ {}^6\mathrm{G}_{11/2}$	474.240	727 (2)	
		486.896	726 (2)	
19 291.57	$4d^3 5s5p\ {}^6\mathrm{G}_{13/2}$	491.092	739 (2)	
19 993.78	$4d^3 5s5p\ {}^6\mathrm{D}_{5/2}$	912.938	827 (3)	
20 315.74	$4d^3 5s5p\ {}^6\mathrm{D}_{7/2}$	925.130	786 (5)	
20 837.98	$4d^3 5s5p\ {}^4\mathrm{D}_{5/2}$	672.19	803 (6)	
20 939.92	$4d^3 5s5p\ {}^6\mathrm{F}_{11/2}$	502.634	756 (4)	
23 022.56	$4d^3 5s5p\ {}^4\mathrm{G}_{7/2}$	908.486	430 (40)*	
23 243.87	$4d^3 5s5p\ {}^4\mathrm{F}_{3/2}$	912.507	0 (30)*	
23 525.80	$4d^4 5p\ {}^2\mathrm{D}_{3/2}$	661.415	595 (7)	
23 574.14	$4d^3 5s5p\ {}^4\mathrm{F}_{5/2}$	918.695	515.7 (8)	
		672.362	514.5 (9)	[1]
24 015.11	$4d^3 5s5p\ {}^4\mathrm{F}_{7/2}$	919.762	595 (5)	
27 855.13	$4d^3 5s5p\ {}^2\mathrm{G}_{7/2}$	914.131	439.1 (7)	
30 940.02	$J = 9/2$	499.428	0 (50)*	
		502.475	0 (50)*	
		507.676	0 (30)*	
31 907.74	$4d^4 5p\ {}^4\mathrm{F}_{3/2}$	502.637	820 (60)*	
32 572.72	$4d^3 5s5p\ {}^4\mathrm{G}_{11/2}$	474.968	0 (20)*	
32 802.44	$4d^4 5p\ {}^4\mathrm{G}_{9/2}$	483.760	613.7 (1.5)	
		570.615	632.5 (3.0)	[10]
38 448.77	$4d^3 5s5p\ {}^2\mathrm{H}_{9/2}$	476.678	390 (50)*	

* B constants of both levels fixed during the fit.

of the peaks. Two levels of even and three of odd parity, investigated in the present work, are such weakly splitting levels. Eight lines are measured to these five weakly splitting levels. For all these lines the B values of both levels are fixed to zero during the fit. The determination of the hyperfine A constants of the second level in each transition also is affected. Consequently, in Tables 2 and 3 eight levels of the each opposite parity also have a high value of the margin of error of A (marked with an asterix).

As examples for the experimental spectra, the partly resolved line of the transition $4d^4 5s\ {}^6\mathrm{D}_{9/2} \longrightarrow 4d^3 5s5p\ {}^6\mathrm{F}_{11/2}$ at $\lambda_{\mathrm{air}} = 502.634$ nm as well as the transition with a weakly splitting level $4d^4 5s\ {}^4\mathrm{H}_{13/2} \longrightarrow 4d^3 5s5p\ {}^4\mathrm{G}_{11/2}$ at $\lambda_{\mathrm{air}} = 474.968$ nm are shown in Figure 1.

In the left spectrum (Fig. 1a) six of the strong hyperfine peaks with $\Delta F = \Delta J = 1$ are resolved, whereas the

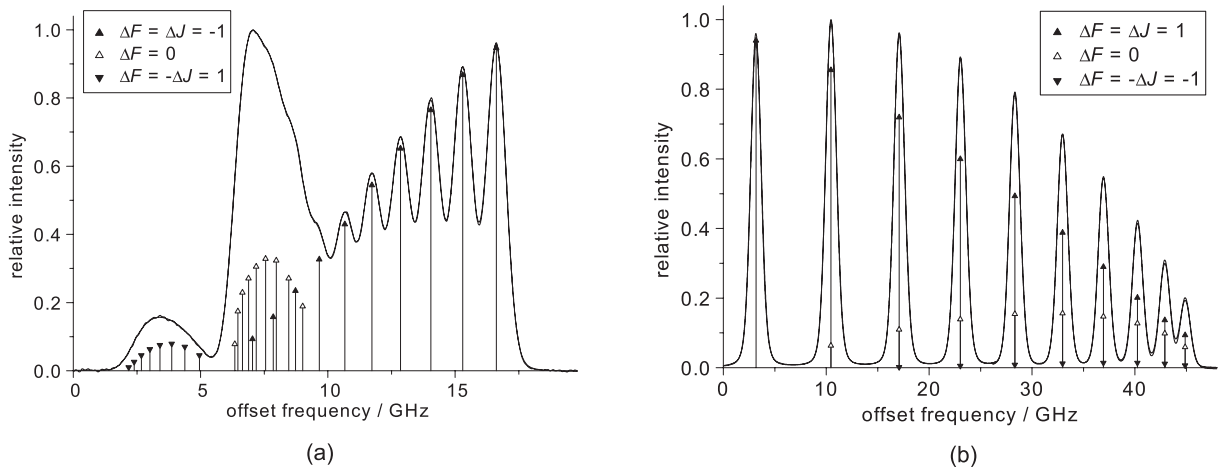

Fig. 1. Hyperfine spectrum of the Nb I lines measured with laser induced fluorescence spectroscopy together with the best fitted curve for the transitions: (a) $4d^4 5s\ ^6\mathrm{D}_{9/2} \longrightarrow 4d^3 5s5p\ ^6\mathrm{F}_{11/2}$ at $\lambda_{\mathrm{air}} = 502.634$ nm, (b) $4d^4 5s\ ^4\mathrm{H}_{13/2} \longrightarrow 4d^3 5s5p\ ^4\mathrm{G}_{11/2}$ at $\lambda_{\mathrm{air}} = 474.968$ nm, the hyperfine components are marked by the difference ΔF of the total angular momenta of the lower and upper hyperfine levels.

remaining hyperfine transitions form two groups of unresolved peaks. In this case, the intensities and line shape parameters of each group with the same ΔF are coupled together.

In the right spectrum (Fig. 1b) the transitions from different upper hyperfine levels to the same lower level lie at the same position. Compared to the peak of the strongest hyperfine component, which is separated, no broadening of the peaks containing two or three hyperfine transitions is detected, and no asymmetry is observed. These facts give evidence of a very small splitting of the upper level in this case.

In Tables 2 and 3, additional to the results of this work, comparative literature values are listed (only reference values of levels investigated in the present work are listed, for details of all hyperfine structure data see [1]). With one exception, the hyperfine structure constants determined in the present work agree within the limit of error with previous values. This exception refers to the levels 32 802.44 cm^{-1}, the comparative value is given in reference [10]. Nor reason is found for this discrepancy.

Finally, calculated values A_{calc} resulting from a parametric analysis of the even configurations [2] are compared in Table 4 with the experimental results. Most of the calculated values are in good agreement with the experimental results. The level 12692.12 cm^{-1} shows the strongest deviation (500 MHz), which is attributed as a disturbance of the fine structure wave functions, as the neighbouring level shows also a strong deviation having a different sign (see [2]).

Table 4. Comparison of the experimental A values, determined in the present work, with calculated values, resulting from a parametric analysis of the even configurations [2]; all values in MHz; * A value already known before and added to the parametric analysis in [2].

E/cm^{-1}	level		A	A_{calc}	ΔA
1 050.26	$4d^4 5s$	$^6\mathrm{D}_{9/2}$	693	684	9*
5 965.45	$4d^3 5s^2$	$^4\mathrm{P}_{5/2}$	342	435	–93*
8 410.90	$4d^4 5s$	$^4\mathrm{D}_{1/2}$	2 001	2 022	–21*
9 043.14	$4d^4 5s$	$^4\mathrm{D}_{5/2}$	–408	–394	–14
9 497.52	$4d^4 5s$	$^4\mathrm{D}_{7/2}$	–477	–496	19
10 922.74	$4d^4 5s$	$^4\mathrm{H}_{7/2}$	–200	–244	44
11 044.08	$4d^4 5s$	$^4\mathrm{H}_{9/2}$	334	196	138
11 247.88	$4d^4 5s$	$^4\mathrm{H}_{11/2}$	560	461	99
11 524.65	$4d^4 5s$	$^4\mathrm{H}_{13/2}$	662	669	–7
12 018.25	$4d^4 5s$	$^4\mathrm{G}_{5/2}$	57	–4	61*
12 136.86	$4d^4 5s$	$^4\mathrm{G}_{7/2}$	502	371	131
12 288.25	$4d^4 5s$	$^4\mathrm{F}_{3/2}$	–590	–599	9
12 692.12	$4d^4 5s$	$^4\mathrm{F}_{5/2}$	339	–179	518
13 145.71	$4d^4 5s$	$^4\mathrm{F}_{9/2}$	667	673	–6
16 918.78	$4d^4 5s$	$^2\mathrm{G}_{7/2}$	–86	–195	109
17 476.22	$4d^4 5s$	$^2\mathrm{H}_{11/2}$	–20	–117	97
37 871.30	$4d^3 5s6s$	$^6\mathrm{F}_{1/2}$	–1 750	–1 750	0*
38 021.41	$4d^3 5s6s$	$^6\mathrm{F}_{3/2}$	552	552	0*
38 276.59	$4d^3 5s6s$	$^6\mathrm{F}_{5/2}$	870	868	2*
38 638.47	$4d^3 5s6s$	$^6\mathrm{F}_{7/2}$	957	958	–1*
39 100.73	$4d^3 5s6s$	$^6\mathrm{F}_{9/2}$	983	983	0*
39 648.67	$4d^3 5s6s$	$^6\mathrm{F}_{11/2}$	994	979	15

4 Conclusion

Optogalvanic and laser induced fluorescence spectroscopy in a hollow cathode discharge have been performed to the determine the magnetic dipole hyperfine structure A constants of 22 levels of even and 21 levels of odd parity of Nb I. For 30 of these 43 levels, the hyperfine structure has been experimentally investigated for the first time with an accuracy of the A constants in the order of MHz. For eight levels of each parity, the accuracy of the A constants is diminished due to a weakly splitting level involved in the investigated transitions. In order to obtain a higher precision for the magnetic dipole constants A of these weakly

splitting levels as well as a determination of the electric quadrupole B constants Doppler-free experimental methods are recommended.

In particular for the levels of odd parity, the number of levels, for which hyperfine structure data are available, is greatly extended by the present work. A parametric analysis of the fine and hyperfine structure of the configurations of odd parity, based on the new information about the fine structure given in [3] and the hyperfine data given in [1] and in the present work is presented in the subsequent paper [11].

References

1. A. Bouzed, S. Kröger, D. Zimmermann, H.-D. Kronfeldt, G. Guthöhrlein, Eur. Phys. J. D **23**, 57 (2003)
2. S. Kröger, A. Bouzed, Eur. Phys. J. D **23**, 63 (2003)
3. S. Kröger, O. Scharf, G. Guthöhrlein, Europhys. Lett. **66**, 344 (2004)
4. C.E. Moore, *Atomic energy levels*, Volume II, NSRDS-NBS 35 (1952)
5. W.F. Meggers, C.H. Corliss, B.F. Scribner, *Tables of spectral line intensities, part I, arranged by elements*, 2nd edn. (National Bureau of Standards, Washington, DC 1975)
6. F.M. Phelps, *M.I.T. Wavelength Tables, Volume 2: Wavelength by element* (The MIT Press, Cambridge, Mass. London, 1991)
7. S. Büttgenbach, R. Dicke, H. Gebauer, M. Herschel, G. Meisel, Z. Phys. A **275**, 193 (1975)
8. L. Fraenkel, C. Bengtsson, D. Hanstrop, A. Nyberg, J. Persson, Z. Phys. D **8**, 171 (1988)
9. R. Singh, G.N. Rao, Phys. Scripta **40**, 170 (1989)
10. R. Singh, R.K. Thareja, G.N. Rao, J. Opt. Soc. Am. B **9**, 493 (1992)
11. S. Kröger et al., Eur. Phys. J. D **41**, 61 (2007)